J Mater Sci (2008) 43:6771–6776
DOI 10.1007/s10853-008-2946-x

Influence of ZrO_2 addition on the structure, thermal stability, and dielectric properties of $ZnTiO_3$ ceramics

Yin-Lai Chai · Yee-Shin Chang · Lay-Gaik Teoh · Yi-Jing Lin · Yu-Jen Hsiao

Received: 16 October 2007 / Accepted: 12 August 2008 / Published online: 17 September 2008

Abstract The zinc titanates doped with zirconium were synthesized by conventional solid-state reaction using metal oxides. X-ray diffractometry and differential scanning calorimetry analysis results indicated that the stable region of the hexagonal $Zn(Zr_xTi_{1-x})O_3$ phase extended to a high temperature (above 945 °C). The c/a value decreased as the Zr concentrations increased, which may be caused by the Zr^{4+} addition resulting in a shorter distance between the center ion and its nearest neighbors of the octahedron, and the bonding force between the B-site ion and oxygen ion of ABO_3 perovskite-like structure becoming stronger. The dielectric properties exhibited a significant dependence on the sintering temperatures and the amount of ZrO_2 addition. The dielectric constant decreased and Curie temperature (T_c) increased slightly with the increasing amounts of Zr ions. This is caused by the second phase of $ZnZrO_3$ which was deposited at the grain boundaries and inhibited the grain growth. Furthermore, diffuse phase transition with a maximum permittivity at a transition temperature that is close to room temperature in $Zn(Zr_xTi_{1-x})O_3$ was observed.

Y.-L. Chai
Department of Resources Engineering, Dahan Institute of Technology, Hualien 971, Taiwan

Y.-S. Chang
Department of Electronic Engineering, National Formosa University, Huwei, Yunlin 632, Taiwan

L.-G. Teoh (✉)
Department of Mechanical Engineering, National Pingtung University of Science and Technology, Neipu, Pingtung 912, Taiwan
e-mail: n5888107@mail.npust.edu.tw

Y.-J. Lin
Department of Materials Science and Engineering, National Cheng Kung University, Tainan 701, Taiwan

Y.-J. Hsiao
National Nano Device Laboratories, Science-based Industrial Park, Hsinshi, Tainan 744, Taiwan

Introduction

Titanate-based perovskite-type oxides, ($MTiO_3$), containing metals such as M = Pb, Ba, Sr, Cd, Fe, and Zn are well known as functional inorganic materials, having wide applications in electrodes of solid oxide fuel cells (SOFC's) [1], metal-air barriers [2], gas sensors [3], microelectronics [4], and high performance catalysts [5] for the complete oxidation of hydrocarbons or CO and NO reduction. Several fundamental studies concerning the phase diagram and the characterization of the ZnO–TiO_2 system have been published since the 1960s [6, 7]. It has been reported that three compounds exist in the ZnO–TiO_2 system [8], Zn_2TiO_4 (cubic), $ZnTiO_3$ (hexagonal), and $Zn_2Ti_3O_8$ (cubic).

$ZnTiO_3$ is an ilmenite titanate with an ordered corundum structure, where each TiO_6 octahedron layer is sandwiched between two layers of MO_6 octahedra. For every octahedron, faces are shared along the c-axis, edges are shared in the ab-plane, and apices are shared along the oblique direction [9]. $ZnTiO_3$ could be used as white pigment [10], a catalytic sorbent for the desulfurization of hot coal gases [11], and as a gas sensor [3] (for ethanol, NO, CO, etc.). Recent works have demonstrated that it is also a useful candidate for microwave resonator materials and suitable for low temperature co-fired ceramics [12]. Research has also indicated that doped and undoped $ZnTiO_3$ have V-type resistivity-temperature characteristics and possess typical PTCR properties above the transition point [13, 14]. In addition, $ZnTiO_3$ doped with

some transition metal ions could be used for luminescence, as proposed by Wang et al. [15, 16].

Since Zirconium is known as an effective substituent in $BaTiO_3$ to shift the Curie temperature downward and raise the other two phase transition temperatures, many investigations have focused on the effect of Zr^{4+} ion additions. Hennings et al. [17]. found that the relative permittivity-temperature plot would give a single broad Curie peak with the addition of the appropriate amount of Zr ions. Further studies of the Zr^{4+}-doped $Ba_{0.4}Sr_{0.4}Ca_{0.2}TiO_3$ system also found that some Zr ions were deposited at grain boundaries to inhibit the grain growth, and one third of the oxygen positions would become occupied, corresponding to a defective pyrochlore structure [18, 19].

There are various methods to prepare $ZnTiO_3$ powders, including conventional solid-state reaction [7] and sol-gel method [8, 20]. Since there are some drawbacks to the sol-gel method, such as the complicated process and the expensive starting agents, the solid-state reaction will be adopted in this paper. The authors have synthesized $ZnTiO_3$ doped with four valance elements replacing titanium by milling the mixture of ZrO_2 and TiO_2 powders using a conventional solid-state reaction. The phases, thermal stability, and dielectric properties of the resulting $Zn(Zr,Ti)O_3$ were then examined.

Experimental procedures

Sample preparation

The $Zn(Zr_xTi_{1-x})O_3$ samples with $x = 0$–0.1 were prepared by a conventional solid-state reaction method using ZnO, TiO_2, and ZrO_2 powders as the starting materials with a purity of 99.99% supplied from Aldrich Chemical Company and Acros Organics. The starting materials were mixed in ethanol by ball milling with zirconia balls in polyethylene jars for 24 h, and then dried at 120 °C. The mixed powders were calcined at 800 °C for 24 h to form the $ZnTiO_3$ phase and further milled for 24 h, also with zirconia balls in polyethylene jars after furnace cooling. The ground powders obtained were then added to 3 wt% of polyvinyl alcohol (PVA) solution as a binder. After drying at 120 °C, they were pressed into disks of 10 mm in diameter and 5 mm thick (with a pressure of about 5 MPa), followed by cold isostatic pressing of 200 MPa for 20 min in rubber bags. Finally the disks were sintered at temperatures of 800–950 °C for 24 h.

Characterizations

The crystal structures were analyzed by X-ray diffractometry (XRD, Rigaku Dmax–33 X-ray diffractometer) using Cu-Kα radiation with 2θ from 20° to 60° to identify the possible phases formed after heat treatment. Differential scanning calorimetry measurements were carried out in a HT-DSC (DSC, Model 404, Netzsch Inc., Exton, PA) equipment to determine the thermal behavior of powders which were placed inside the closed platinum cups and measured at a rate of 10 °C/min in a dry nitrogen (99.99%) atmosphere. For examination of the dielectric properties, both sides of the specimens were finished to a mirror surface, and electrodes were attached to the surfaces using ohmic silver paste and gold wires. Temperature dependence of the dielectric constant (ε) was measured with an inductance–capacitance–resistance (LCR) (Hewlett-Packard, HP–4284A) meter at 1 kHz between −10 and 70 °C by heating and cooling the sample at a rate of 4 °C/min. The sintered density and open porosity were calculated using the Archimedes method [21].

Results and discussion

Phases in samples

Figure 1 shows the XRD profiles for the zinc titanate doped with 1 at% zirconium oxide sintered at different temperatures from 800 to 950 °C for 24 h in air. The almost pure

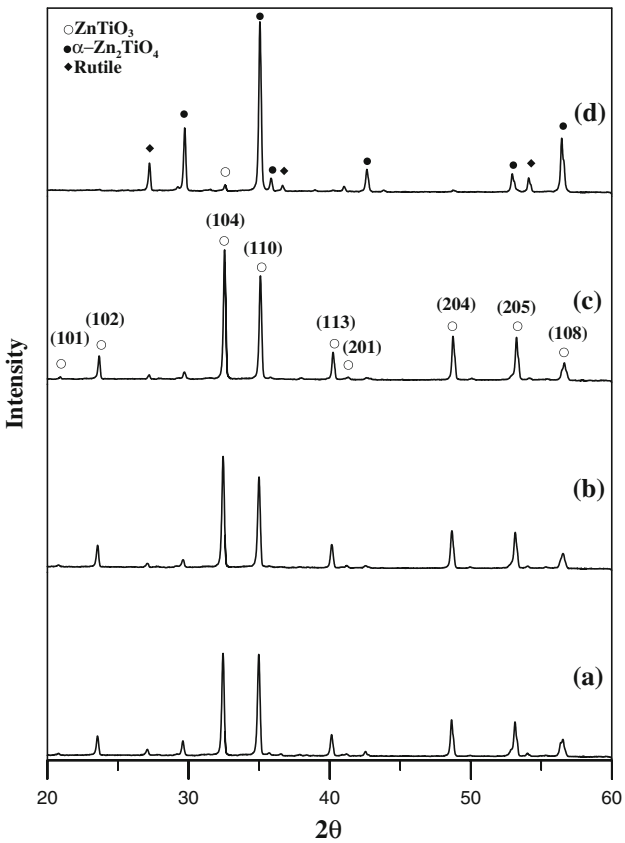

Fig. 1 XRD profile of $ZnTiO_3$ doped with 1 at% Zr after heat treatment at (**a**) 800, (**b**) 850, (**c**) 900, and (**d**) 950 °C for 24 h in air

$ZnTiO_3$ phase was observed in the variation of the temperatures from 800 to 900 °C [JCPDS No.14-0033]. This means that the zirconia ion can permeate into the lattice of the $ZnTiO_3$ structure and replace one of the titanium ions to form the solid solution of $Zn(Zr,Ti)O_3$. The half-peak width seems to narrow with increasing the sintering temperatures, because a higher sintering temperature favors a crystal structure with a larger crystalline size which leads to a better crystallinity. When the sintering temperature was increased to 950 °C, which is higher than the decomposition temperature of $ZnTiO_3$ (945 °C), the amount of α-Zn_2TiO_4 and rutile phases were increased, and only one small peak of $ZnTiO_3$ phase remained near the diffraction angle of 32°, designated as (104). Figure 2 shows the XRD profiles of $ZnTiO_3$ doped with (a) 1, (b) 3, (c) 5, (d) 10 at% Zr sintered at 950 °C for 24 h in air. The $ZnTiO_3$ phase still existed even though the sintering temperature was higher than the decomposition temperature of $ZnTiO_3$ (945 °C). The α-Zn_2TiO_4 and rutile phases reduced gradually and the amount of $ZnZrO_3$ increased with Zr concentration. The Zr that dissolved in $ZnTiO_3$ seemed to have a limit up to 5 at%, where a small peak of $ZnZrO_3$ appeared at 10 at% of Zr doped. Based on the XRD analysis, the addition of Zr can raise the decomposition

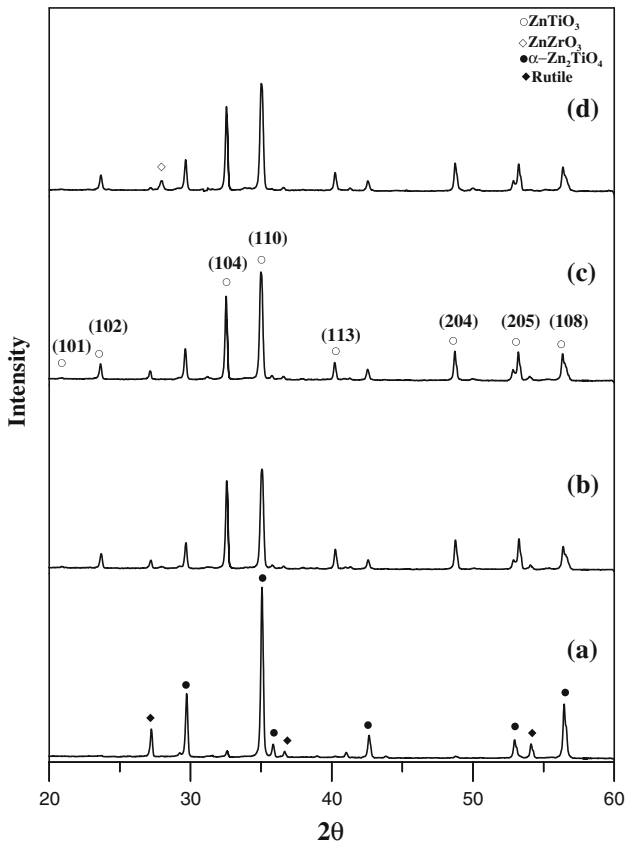

Fig. 2 XRD profile of $ZnTiO_3$ doped with (**a**) 1, (**b**) 3, (**c**) 5, and (**d**) 10 at% Zr after heat treatment at 950 °C for 24 h in air

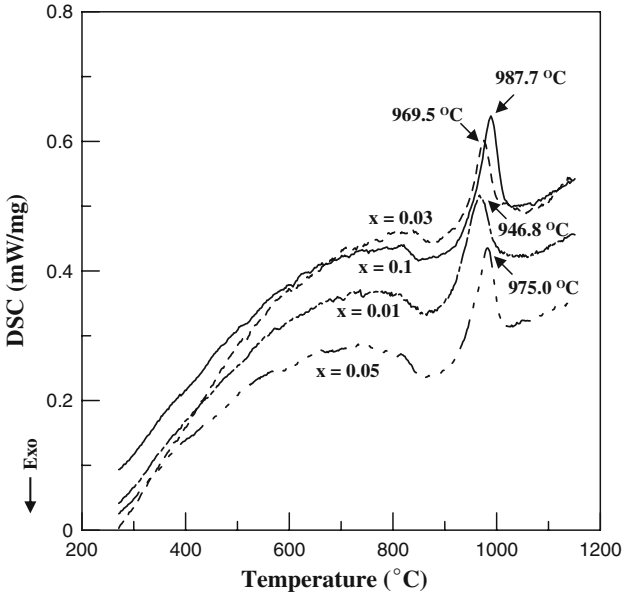

Fig. 3 The DSC curves of $Zn(Zr_xTi_{1-x})O_3$ powders

temperature of $ZnTiO_3$. To examine the thermal stability of $Zn(Zr,Ti)O_3$, high temperature differential scanning calorimetry (DSC) was employed, and the resulting curves are plotted in Fig. 3. It is obvious that Zr improves the stability of the $ZnTiO_3$ structure. The endothermic peaks, designated as thermal decomposition temperature, clearly shifted from 946.8 °C to 987.7 °C with the increasing concentrations of Zr from 1 to 10 at%, respectively. Table 1 shows the parameters of $ZnTiO_3$ doped with different amounts of Zr sintered at 900 °C for 24 h in air. The lattice constants were determined from the diffraction patterns using a computer program called *Unit Cell*. Table 1 indicates that the c/a value decreases as the Zr concentrations increases, which may be the reason the Ti^{4+} ion (0.68 Å) is substituted by the Zr^{4+} ion (0.87 Å), resulting in a shorter distance between the center ion and its nearest neighbors of the octahedron. This substitution caused the bonding force between the B-site ion and oxygen ion of ABO_3 perovskite-like structure to become stronger and led the decomposition temperature to increase.

Table 1 The parameters of $Zn(Ti_{1-x}Zr_x)O_3$ sintered at 900 °C for 24 h in air

Sample	Porosity (%)	Sintered density (g/cm^3)	T_c (°C)	c/a
$ZnTiO_3$	34.62	3.370	~5.0	2.7349
$Zn(Zr_{0.01}Ti_{0.99})O_3$	40.70	3.056	~11.5	2.7345
$Zn(Zr_{0.03}Ti_{0.97})O_3$	41.06	3.050	~12.0	2.7338
$Zn(Zr_{0.05}Ti_{0.95})O_3$	41.30	3.041	~13.0	2.7329
$Zn(Zr_{0.10}Ti_{0.90})O_3$	41.99	3.028	~13.5	2.7326

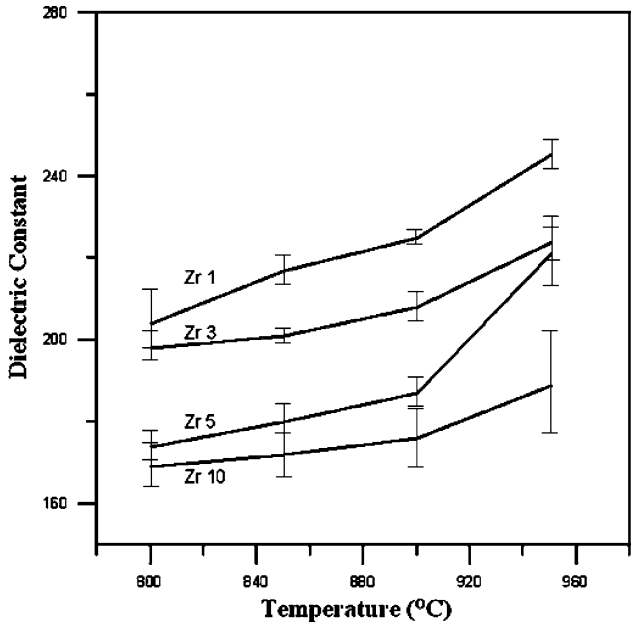

Fig. 4 The dielectric constants of $ZnTiO_3$ doped with different concentrations of Zr sintered at various temperatures

Dielectric properties

The dielectric properties of pure zinc titanate ceramics were investigated by Sugiura and Ikeda [22]. They measured the low frequency (kHz) dielectric constants and found the temperature coefficient of the dielectric constant $\tau_\varepsilon = 0$ for the composition containing 53 at% ZnO. The dielectric constants of $ZnTiO_3$ doped with different concentrations of Zr measured at a frequency of 1 kHz for various sintering temperatures are illustrated in Fig. 4. The dielectric constants did not show much difference between the samples sintered at 800 and 900 °C. They increased slightly with the increasing sintering temperature, and had a low value compared with that of perovskite titanate compounds such as $CaTiO_3$ or $SrTiO_3$ [23]. It has been reported that the TiO_6 octahedral in ilmenite titanate is isolated by both the MO_6 octahedral layer and cation vacancy layer, leading to a decrease in the cooperative interaction between the TiO_6 octahedra [9]. In addition, there is a distinct decrease for dielectric constants of the $ZnTiO_3$ doped with different concentrations of Zr, which is because the porosity increases with increasing the Zr concentration.

Figure 5a and b shows the temperature dependence on dielectric constants and dissipation factors for $ZnTiO_3$ doped with different concentrations of Zr sintered at 900 °C at 1 kHz. In fact, the Curie temperature (T_c) is not sensitive to Zr concentration, but it seems to increase slightly from 11.5 °C for 1 at% Zr to 13.5 °C for 5 at% Zr doping. As mentioned above, each TiO_6 octahedron layer is sandwiched between two layers of MO_6 octahedra. In

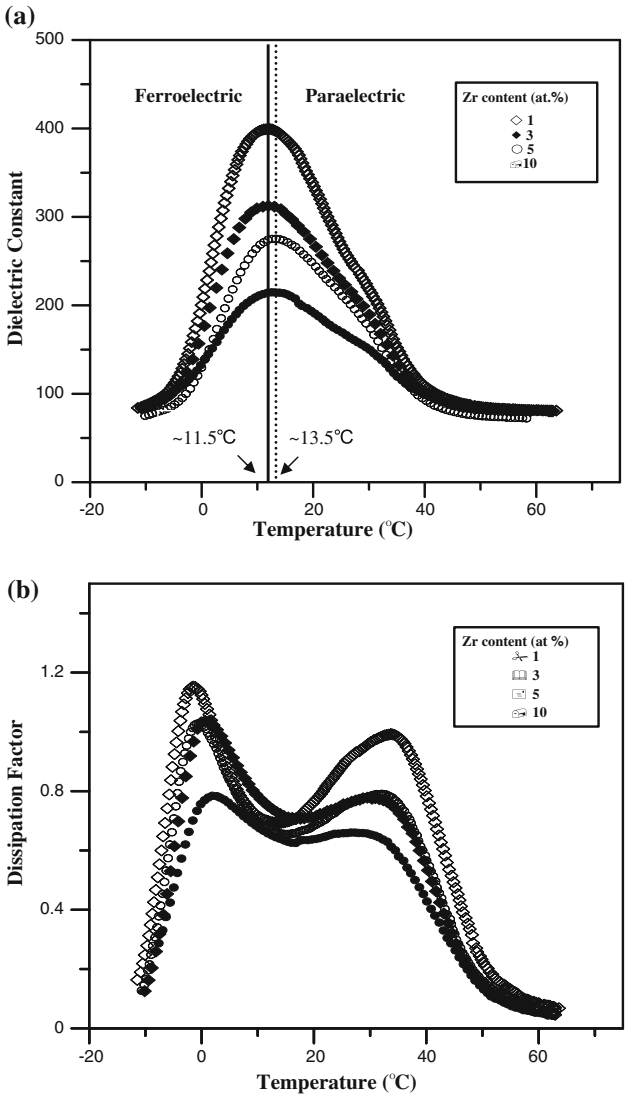

Fig. 5 The dielectric constant (**a**) and dielectric loss (**b**) at 1 kHz as a function of temperature for $ZnTiO_3$ doped with different concentrations of Zr sintered at 900 °C

every octahedron, faces are shared along the c-axis, edges are shared in the ab-plane, and apices are shared along the oblique direction. One pair of edge-shared TiO_6 octahedra is isolated by the cation vacancies in the ab-plane and is separated by the MO_6 octahedron along the oblique direction [9]. When $ZnTiO_3$ was doped with Zr^{4+} to substitute the Ti^{4+} ions, the distance between every TiO_6 octahedron layer decreased and the interaction between TiO_6 octahedron layers was enhanced, which may increase the Curie temperature (T_c).

The dielectric peak is broadened because of the compositional fluctuation and/or substitution disordering in the arrangement of cations in one or more crystallographic sites of the structure. This leads to the microscopic heterogeneity in the compounds, which is distributed at different

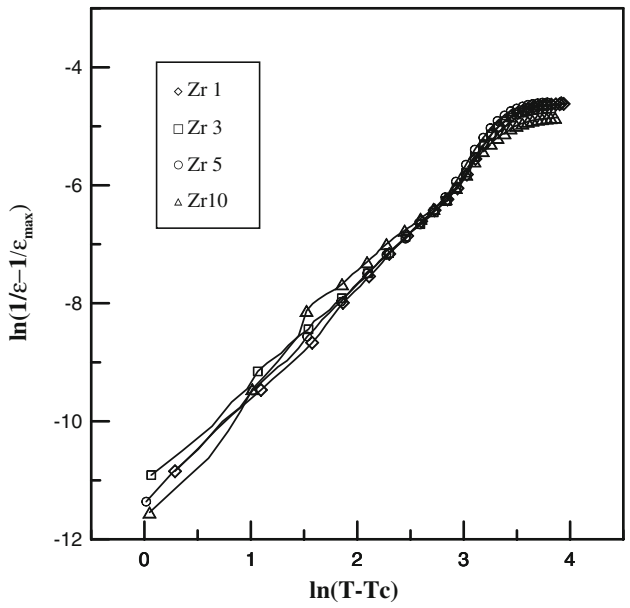

Fig. 6 Variation of $\ln(1/\varepsilon - 1/\varepsilon_{max})$ versus $\ln(T - T_c)$ of $Zn(Zr_xTi_{1-x})O_3$ above T_c

local Curie points [24]. The quantitative assessment of the diffusivity (γ) of the broadened peak in the paraelectric phase was evaluated using the expression of $\ln(1/\varepsilon - 1/\varepsilon_{max})$ vs. $(T - T_c)^{\gamma}$ [25]. The plots of $\ln(1/\varepsilon - 1/\varepsilon_{max})$ vs. $(T - T_c)$ for all compositions are represented in Fig. 6. The value of γ was found to be between 1 (normal Curie-Weiss behavior) and 2 (completely disordered), which confirms that diffuse phase transition occurred in the materials. This shows that an increase in diffuseness of the materials is a function of Zr ion doping. The deviation of the phase transition mechanism from the Curie-Weiss type can be interpreted as the occurrence of disorder in the system. Furthermore, the dielectric constant decreased by increasing the concentrations of Zr due to the effect of the decrease of grain size and substantial replacement of Ti^{4+} ions by Zr^{4+} ions in the perovskite structure [26]. An earlier report [17] also indicated that in some perovskite materials the grain sizes decreased with the increasing amounts of Zr, because some Zr ions migrated to grain boundaries and inhibited grain growth. $Zn(Zr_xTi_{1-x})O_3$ has the M-type dissipation factor-temperature characteristics (Fig. 5b), and these diminish by increasing the amount of Zr. As mentioned above, with the decrease in grain size the degree of spontaneous polarization decreased, and the energy needed for dipoles to revolve under the effect of electric field was lowered [27].

Conclusions

The crystal structures, thermal stability, and dielectric properties of $ZnTiO_3$ doped with different concentrations of Zr have been investigated. As doping concentrations of Zr increased from 1 to 10 at%, the decomposition of $ZnTiO_3$ could be suppressed more and the stable region of the hexagonal $Zn(Zr_xTi_{1-x})O_3$ phase extended from 946.8 °C to 987.7 °C. The coexistence of mixture phases clearly improved dielectric constants when the sintering temperature was 950 °C. In addition, there is a limit for the $Zn(Zr_xTi_{1-x})O_3$ solid solution, and the value is about $x = 5$ at%. The increased electronic polarizability of Zr^{4+} might raise the Curie temperature (T_c) initially, but the solution limit of Zr in $Zn(Zr_xTi_{1-x})O_3$ would satisfy the Curie temperature. Moreover, some $ZnZrO_3$ are deposited at grain boundaries to inhibit the grain growth, which lets the dielectric constants and dissipation factors decrease with a maximum permittivity at a transition temperature that is close to room temperature.

Acknowledgements The authors wish to thank the Nation Science Council of Taiwan for supporting the project with grant number NSC96-2622-E-150-034-CC3.

References

1. Yamamoto O, Takeda Y, Kanno R, Noda M (1987) Solid State Ionic 22:241. doi:10.1016/0167-2738(87)90039-7
2. Shimizu Y, Uemura K, Miura N, Yamzoe N (1988) Chem Lett 12:1979. doi:10.1246/cl.1988.1979
3. Obayashi H, Sakurai Y, Gejo T (1976) J Solid State Chem 17:299. doi:10.1016/0022-4596(76)90135-3
4. Shimizu Y, Komatsu H, Michishita S, Miura M, Yamazoe N (1996) Sens Actuators B 34:493. doi:10.1016/S0925-4005(97)80021-4
5. Chen ZX, Derking A, Koot W, van Dijk MP (1996) J Catal 161:730. doi:10.1006/jcat.1996.0235
6. Dulin FH, Rase DE (1960) J Am Ceram Soc 43:125. doi:10.1111/j.1151-2916.1960.tb14326.x
7. Bartram SF, Slepetys RA (1961) J Am Ceram Soc 44:493. doi:10.1111/j.1151-2916.1961.tb13712.x
8. Yamaguchi O, Morimi M, Kawabata H, Shimizu K (1987) J Am Ceram Soc 70:c97
9. Sohn JH, Inaguma Y, Yoon SO, Itoh M, Nakamura T, Yoon SJ, Kim HJ (1994) Jpn J Appl Phys 33:5466. doi:10.1143/JJAP.33.5466
10. McCord AT, Saunder HF (1945) Ceram Abstr. US Patent 2,739,019
11. Ozdemir S, Bardakci T (1999) Sep Purif Technol 16:225. doi:10.1016/S1383-5866(99)00013-1
12. Kim HT, Nahm S, Byun JD (1999) J Am Ceram Soc 82(12):3476
13. Chang YS, Chang YH, Chen IG, Chen GJ, Chai YL, Wu S, Fang TH (2003) J Alloy Compd 354:303
14. Chang YS, Chang YH, Chen IG, Chen GJ (2003) Solid State Commun 128:203. doi:10.1016/S0038-1098(03)00527-1
15. Wang SF, Gu F, Lü MK, Song CF, Xu D, Yuan DR, Liu SW (2003) Chem Phys Lett 373:223. doi:10.1016/S0009-2614(03)00620-1
16. Wang SF, Lü MK, Gu F, Song CF, Xu D, Yuan DR, Liu SW, Zhou GJ, Qi YX (2003) Inorg Chem Commun 6:185. doi:10.1016/S1387-7003(02)00711-6
17. Hennings D, Schnell A, Simon G (1982) J Am Ceram Soc 65:539. doi:10.1111/j.1151-2916.1982.tb10778.x

18. Lee SG, Kang DS (2003) Mater Lett 57:1629. doi:10.1016/S0167-577X(02)01043-1
19. Glerup M, Nielsen OF, Poulsen FW (2001) J Solid State Chem 160:25. doi:10.1006/jssc.2000.9142
20. Chang YS, Chang YH, Chen IG, Chen GJ, Chai YL (2002) J Cryst Growth 243:319. doi:10.1016/S0022-0248(02)01490-2
21. Doerr W, Assmann H, Maier G, Steven J (1979) J Nucl Mater 81:135. doi:10.1016/0022-3115(79)90071-0
22. Sugiura M, Ikeda K, (1950) J Jpn Ceram Assoc 55 (626) 62; Ceram Abstr 164e
23. Lemanov VV, Sotnikov AV, Smirnova EP, Weihnacht M, Kunze R (1999) Solid State Commun 110:611. doi:10.1016/S0038-1098(99)00153-2
24. Lines ME, Glass AM (1977) Principals and applications of ferroelectrics and related materials. Oxford University Press, Oxford
25. Piligrim SM, Sutherland AE, Winzer SR (1990) J Am Ceram Soc 73:3122. doi:10.1111/j.1151-2916.1990.tb06733.x
26. Jaffe B, Cook WR, Jaffe H (1971) Piezoelectric ceramics. Academic Press, New York, p 98
27. Luan W, Gao L, Guo J (1999) Ceram Int 25:727. doi:10.1016/S0272-8842(99)00009-7